Functional MRI brain state occupancy in the presence of cerebral small vessel disease – a pre-registered replication analysis of the Hamburg City Health Study

Thies Ingwersen, MD [1], **Carola Mayer, PhD** [1], **Marvin Petersen, MD** [1], **Benedikt M. Frey, MD** [1], **Jens Fiehler, MD** [2], **Uta Hanning, MD** [2], **Simone Kühn, PhD** [3,4], **Jürgen Gallinat, MD** [3], **Raphael Twerenbold, MD** [5], **Christian Gerloff, MD** [6], **Bastian Cheng, MD** [1], **Götz Thomalla, MD** [1], **Eckhard Schlemm, MBBS PhD** [1]

[1]Department of Neurology, University Medical Center Hamburg-Eppendorf; [2]Department of Neuroradiology, University Medical Center Hamburg-Eppendorf; [3]Department of Psychiatry, University Medical Center Hamburg-Eppendorf; [4]Max-Planck-Institut für Bildungsforschung, Berlin; [5]Department of Cardiology, University Medical Center Hamburg-Eppendorf; [6]University Medical Center Hamburg-Eppendorf

✉ **For correspondence:**
e.schlemm@uke.de

Present address:
Dr. Dr. Eckhard Schlemm, Klinik und Poliklinik für Neurologie, Universitätsklinikum Hamburg-Eppendorf, Martinistr. 52, D-20251 Hamburg

Abstract

Objective: To replicate recent findings on the association between the extent of cerebral small vessel disease (cSVD), functional brain network dedifferentiation, and cognitive impairment.

Methods: We analyzed demographic, imaging, and behavioral data from the

prospective population-based Hamburg City Health Study. Using a fully prespecified analysis pipeline, we estimated discrete brain states from structural and resting-state functional magnetic resonance imaging (MRI). In a multiverse analysis, we varied brain parcellations and functional MRI confound regression strategies. The severity of cSVD was operationalized as the volume of white matter hyperintensities of presumed vascular origin. Processing speed and executive dysfunction were quantified using the Trail Making Test (TMT).

Hypotheses: We hypothesized a) that a greater volume of supratentorial white matter hyperintensities would be associated with less time spent in functional MRI-derived brain states of high fractional occupancy; and b) that less time spent in these high-occupancy brain states is associated with a longer time to completion in part B of the TMT.

Results: High-occupancy brain states were characterized by activation or suppression of the default mode network. Every 5.1-fold increase in WMH volume was associated with a 0.94-fold reduction in the odds of occupying DMN-related brain states (P 5.01×10^{-8}). Every 5 % increase in time spent in high-occupancy brain states was associated with a 0.98-fold reduction in the TMT-B completion time (P 0.0116). Findings were robust across most brain parcellations and confound regression strategies.

Conclusion: We successfully replicated previous findings on the association between cSVD, functional brain occupancy, and cognition in an independent sample. The data provide further evidence for a functional network dedifferentiation hypothesis of cSVD-related cognitive impairment. Further research is required to elucidate the mechanisms underlying these associations.

Introduction

Cerebral small vessel disease (cSVD) is an arteriolopathy of the brain associated with age and common cardiovascular risk factors (Wardlaw, C. Smith, and Dichgans, 2013). cSVD predisposes patients to ischemic stroke (in particular lacunar stroke) and may lead to cognitive impairment and dementia (Cannistraro et al., 2019). Neuroimaging findings in cSVD reflect its underlying pathology (Wardlaw, Valdés Hernández, and Muñoz-Maniega, 2015) and include white matter hyperintensities (WMH), lacunes of presumed vascular origin, small subcortical infarcts and microbleeds, enlarged perivascular spaces as well

as brain atrophy (Wardlaw, E. E. Smith, et al., 2013). However, the extent of visible cSVD features on magnetic resonance imaging (MRI) is an imperfect predictor of the severity of clinical sequelae (Das et al., 2019) and our understanding of the causal mechanisms linking cSVD-associated brain damage to clinical deficits remains limited (Bos et al., 2018).

Recent efforts have focused on exploiting network aspects of the structural (Tuladhar, Dijk, et al., 2016; Tuladhar, Tay, et al., 2020; Lawrence, Zeestraten, et al., 2018) and functional (Dey et al., 2016; Schulz et al., 2021) organization of the brain to understand the relationship between cSVD and clinical deficits in cognition and other domains that rely on distributed processing. Reduced structural network efficiency has repeatedly been described as a causal factor in the development of cognitive impairment, particularly executive dysfunction and reduced processing speed in cSVD (Lawrence, Chung, et al., 2014; Shen et al., 2020; Reijmer et al., 2016; Prins et al., 2005). Findings with respect to functional connectivity (FC), however, are more heterogeneous than their SC counterparts, perhaps because FC measurements are prone to be affected by hemodynamic factors and noise, resulting in relatively low reliability, especially with resting-state scans of short duration (Laumann, Gordon, et al., 2015). This problem is exacerbated in the presence of cSVD and worsened by arbitrary processing choices (Lawrence, Tozer, et al., 2018; Gesierich et al., 2020).

As a promising new avenue, time-varying, or dynamic, functional connectivity approaches have recently been explored in patients with subcortical ischemic vascular disease (Yin et al., 2022; Xu et al., 2021). Although the study of dynamic FC measures may not solve the problem of limited reliability, especially in small populations or ~~subjects~~ participants with extensive structural brain changes, it adds another – temporal – dimension to the study of functional brain organization, which is otherwise overlooked. Importantly, FC dynamics not only reflect moment-to-moment fluctuations in cognitive processes, but are also related to brain plasticity and homeostasis (Laumann and Snyder, 2021; Laumann, Snyder, et al., 2017), which may be impaired in cSVD.

In the present paper, we aimed to replicate and extend the main results of (Schlemm et al., 2022). In this recent study, the authors analyzed MR imaging and clinical data from the prospective Hamburg City Health Study (HCHS, (Jagodzinski et al., 2020)) using a coactivation pattern approach to define discrete brain states and found associations between the WMH load, time spent in high-occupancy brain states characterized by activation or suppression of the default mode network (DMN), and cognitive impairment. Specifically,

every 4.7-fold increase in WMH volume was associated with a 0.95-fold reduction in the odds of occupying a DMN-related brain state; every 2.5 seconds (i.e., one repetition time) not spent in one of those states was associated with a 1.06-fold increase in TMT-B completion times.

The fractional occupancy of a functional MRI-derived discrete brain state is a ~~subject-specific~~ participant-specific measure of brain dynamics and is defined as the proportion of BOLD volumes assigned to that state relative to all BOLD volumes acquired during a resting-state scan.

Our primary hypothesis for the present work was that the volume of supratentorial white matter hyperintensities is associated with fractional occupancy of DMN-related brain states in a middle-aged to elderly population mildly affected by cSVD. Our secondary hypothesis was that fractional occupancy is associated with executive dysfunction and reduced processing speed, measured as the time to complete part B of the Trail Making Test (TMT).

Both hypotheses were tested in an independent subsample of the HCHS study population using the same imaging protocols, examination procedures, and analysis pipelines as those in (Schlemm et al., 2022). The robustness of the associations was explored using a multiverse approach by varying key steps in the analysis pipeline.

Methods

Study population

This study analyzed data from the Hamburg City Health Study (HCHS), an ongoing prospective, population-based cohort study aiming to recruit a cross-sectional sample of 45 000 adult participants from the city of Hamburg, Germany (Jagodzinski et al., 2020). From the first 10 000 participants of the HCHS, we planned to include those who were documented to have received brain imaging (n=2648) and exclude those who were analyzed in our previous report (Schlemm et al., 2022) (n=970). The ethical review board of the Landesärztekammer Hamburg (State of Hamburg Chamber of Medical Practitioners) approved the HCHS (PV5131), and all participants provided written informed consent.

Demographic and clinical characterization

From the study database, we extracted the participants' age at the time of inclusion in years, their sex, and the number of years spent in education. During the visit to the study

center, participants underwent cognitive assessment using standardized tests. From the database, we extracted their performance scores on the Trail Making Test part B, measured in seconds, as an operationalization of executive function and psychomotor processing speed (Tombaugh, 2004; Arbuthnott and Frank, 2000). For descriptive purposes, we also extracted data on past medical history and reported the proportion of participants with a previous diagnosis of dementia.

MRI acquisition and preprocessing

The magnetic resonance imaging protocol for the HCHS includes structural and resting-state functional sequences. The acquisition parameters for a $3\,\mathrm{T}$ Siemens Skyra MRI scanner (Siemens, Erlangen, Germany) have been previously reported (Petersen et al., 2020; Frey et al., 2021) and are given as follows:

For T_1-weighted anatomical images, a 3D rapid acquisition gradient-echo sequence (MPRAGE) was used with the following sequence parameters: repetition time TR = $2500\,\mathrm{ms}$, echo time TE = $2.12\,\mathrm{ms}$, 256 axial slices, slice thickness ST = $0.94\,\mathrm{mm}$, and in-plane resolution IPR = $(0.83 \times 0.83)\,\mathrm{mm}^2$.

T_2-weighted fluid attenuated inversion recovery (FLAIR) images were acquired with the following sequence parameters: TR = $4700\,\mathrm{ms}$, TE = $392\,\mathrm{ms}$, 192 axial slices, ST = $0.9\,\mathrm{mm}$, IPR = $(0.75 \times 0.75)\,\mathrm{mm}^2$.

125 resting state functional MRI volumes were acquired (TR = $2500\,\mathrm{ms}$; TE = $25\,\mathrm{ms}$; flip angle = 90°; slices = 49; ST = $3\,\mathrm{mm}$; slice gap = $0\,\mathrm{mm}$; IPR = $(2.66 \times 2.66)\,\mathrm{mm}^2$). The ~~subjects~~ participants were asked to keep their eyes open and to think of nothing.

We verified the presence and voxel dimensions of expected MRI data for each participant and excluded those for whom at least one of T_1-weighted, FLAIR, and resting-state MRI was missing. We also excluded participants with neuroradiologically confirmed space-occupying intra-axial lesion. To ensure reproducibility, no visual quality assessment of raw images was performed.

For the remaining participants, structural and resting-state functional MRI data was preprocessed using FreeSurfer v6.0 (https://surfer.nmr.mgh.harvard.edu/), and fmriPrep v20.2.6 (Esteban et al., 2019), using default parameters. Participants were excluded if automated processing using at least one of these packages failed.

Quantification of WMH load

For our primary analysis, the extent of ischemic white matter disease was operationalized as the total volume of supratentorial WMHs obtained from automated segmentation using a combination of anatomical priors, BIANCA (Griffanti, Zamboni, et al., 2016), and LOCATE (Sundaresan et al., 2019), post-processed with a minimum cluster size of 30 voxels, as described in (Schlemm et al., 2022). In an exploratory analysis, we partitioned voxels identified as WMH into deep and periventricular components according to their distance to the ventricular system (cut-off $10\,\mathrm{mm}$, (Griffanti, Jenkinson, et al., 2018))

Brain state estimation

The output from fMRIprep was post-processed using xcpEngine v1.2.3 to obtain de-confounded spatially averaged BOLD time series (Ciric, Wolf, et al., 2017). For the primary analysis, we used the *36p* regression strategy and the Schaefer-400 parcellation (Schaefer et al., 2018), as in (Schlemm et al., 2022).

Different atlases and confound regression strategies, as implemented in xcpEngine, were included in an exploratory multiverse analysis.

Co-activation pattern (CAP) analysis was performed by first aggregating parcellated, de-confounded BOLD signals into a $\left(n_{\text{parcels}} \times \sum_i n_{\text{time points},i}\right)$ feature matrix, where $n_{\text{time points},i}$ denotes the number of retained volumes for ~~subject~~ participant i after confound regression. Clustering was performed using the k-means algorithm ($k = 5$) with a distance measure given by 1 minus the sample Pearson correlation between points, as implemented in Matlab R2021a. We estimated the ~~subject~~ participant- and state-specific fractional occupancies, which are defined as the proportion of BOLD volumes assigned to each brain state (Vidaurre et al., 2018). The two states with the highest average occupancies were identified as the basis for further analysis.

Statistical analysis

For demographic (age, sex, and years of education) and clinical (TMT-B) variables, the number of missing items is reported. For non-missing values, we provide descriptive summary statistics using median and interquartile range. The proportions of men and women in the sample are reported. Since we expected based on our pilot data (Schlemm et al., 2022) that the proportion of missing data would be small, primary regression modelling was carried out as a complete-case analysis.

As an outcome-neutral quality check of the implementation of the MRI processing pipeline, brain state estimation, and co-activation pattern analysis, we compared fractional occupancies between brain states. We expected that the average fractional occupancy in the two high-occupancy states would be higher than the average fractional occupancy in the other three states. Point estimates and 95% confidence intervals are presented for the difference in average fractional occupancy to verify this assertion.

For further analyses, non-zero WMH volumes were subjected to logarithmic transformation. Zero values retained their value of zero; to compensate, all models included a binary indicator for zero WMH volume if at least one non-zero WMH value was present.

To assess the primary hypothesis of a negative association between the extent of ischemic white matter disease and time spent in high-occupancy brain states, we performed a fixed-dispersion Beta regression to model the logit of the conditional expectation of the average fractional occupancy of two high-occupancy states as an affine function of the logarithmized WMH load. Age and sex were included as covariates. The strength of the association was quantified as the odds ratio per interquartile ratio of the WMH burden distribution, and is accompanied by a 95% confidence interval. Significance testing of the null hypothesis of no association was conducted at the conventional significance level of 0.05. Estimation and testing were carried out using the 'betareg' package v3.1.4 in R v4.2.1.

To assess the secondary hypothesis of an association between time spent in high-occupancy brain states and executive dysfunction, we performed a generalized linear regression with a Gamma response distribution to model the logarithm of the conditional expected completion time in part B of the TMT as an affine function of the average fractional occupancy of two high-occupancy states. Age, sex, years of education, and logarithmized WMH load were included as covariates. The strength of the association was quantified as a multiplicative factor per percentage point and accompanied by a 95% confidence interval. Significance testing of the null hypothesis of no association was conducted at the conventional significance level of 0.05. Estimation and testing were performed using the glm function included in the 'stats' package from R v4.2.1.

Pre-registered analyses

The analysis plan was ~~pre-restistered~~ pre-registered on June 27 2023 at https://osf.io/fcqmb. The sample size calculation was based on an effect size on the odds ratio scale of 0.95, corresponding to an absolute difference in the probability of occupying a DMN-
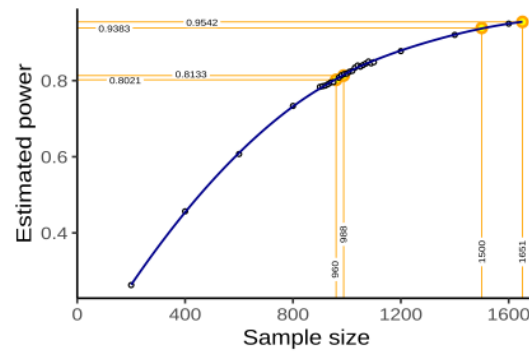
Figure 1 | Sample size and power estimation. A-priori estimated power for different sample sizes was obtained as the proportion of synthetic data sets in which the null hypothesis of no association between WMH volume and time spent in high-occupancy brain states an be rejected at the $\alpha = 0.05$ significance level. Proportions are based on a total of $10\,000$ synthetic data sets obtained by bootstrapping the data presented in (Schlemm et al., 2022). Highlighted in orange are the smallest sample size ensuring a power of at least $80\,\%$ ($n = 960$), the sample size of the pilot data ($n = 988$, post-hoc power $81.3\,\%$), the expected sample sample size for this replication study ($n = 1500$, a-priori power $93.9\,\%$), and the achieved sample size ($n = 1651$, a-priori power $95.4\,\%$).

214 related brain state between the first and third WMH-load quartile of 1.3 percentage

215 points, and between the 5% and 95% percentile of 3.1 percentage points. Approximat-

216 ing half the difference in fractional occupancy of DMN-related states between different

217 task demands (rest vs n-back) in healthy ~~subjects~~participants, which was estimated to

218 lie between 6 and 7 percentage points (Cornblath et al., 2020), this value represented a

219 plausible choice for the smallest effect size of theoretical and practical interest. It also

220 equals the estimated effect size based on the data presented in (Schlemm et al., 2022).

221 Simple bootstrapping was used to create $10\,000$ hypothetical datasets of size 200, 400,

222 600, 800, 900, 910, ..., 1090, 1100, 1200, 1400, 1500, and 1600. Each dataset was then sub-

223 jected to the estimation procedure described above. For each sample size, the propor-

224 tion of datasets in which the primary null hypothesis of no association between fractional

225 occupancy and WMH load could be rejected at $\alpha = 0.05$ was computed and recorded as

226 a power curve in Figure 1.

227 A sample size of 960 would have allowed the replication of the reported effect with a

228 power of $80.2\,\%$. We had anticipated a sample size of 1500, which would have yielded a

229 power of $93.9\,\%$.

Multiverse analysis

231 In both (Schlemm et al., 2022) and our primary replication analysis, we made certain ana-

232 lytical choices in the operationalization of brain states and ischemic white matter disease,

233 namely the use of the *36p* confound regression strategy, the Schaefer-400 parcellation,

234 and a BIANCA/LOCATE-based WMH segmentation algorithm. The robustness of the as-
235 sociation between WMH burden and time spent in high-occupancy states with regard to
236 other choices was explored in a multiverse analysis (Steegen et al., 2016). Specifically, in
237 an exploratory analysis, we estimated brain states from BOLD time series processed ac-
238 cording to a variety of established confound regression strategies and aggregated over
239 different cortical brain parcellations (Table 2, Ciric, Rosen, et al., 2018; Ciric, Wolf, et al.,
240 2017). The extent of cSVD was additionally quantified by the volume of deep and periven-
241 tricular white matter hyperintensities.

242 For each combination of analytical choice of confound regression strategy, parcella-
243 tion, and subdivision of white matter lesion load ($9 \times 9 \times 3 = 243$ scenarios in total), we
244 quantified the association between WMH load and average time spent in high-occupancy
245 brain states using odds ratios and 95% confidence intervals as described above.

246 No hypothesis testing was performed for these multiverse analyses. Rather, they
247 serve to inform about the robustness of the outcome of the test of the primary hypoth-
248 esis. Any substantial conclusions about the association between the severity of cerebral
249 small vessel pathology and the time spent in high-occupancy brain states were drawn
250 from the primary analysis using pre-specified methodological choices, as stated in the
251 Scientific Question in Table 1.

Further exploratory analysis

253 In previous work, two high-occupancy brain states have been related to the default mode
254 network (Cornblath et al., 2020). We further explored this relationship by computing, for
255 each individual brain state, the cosine similarity of the positive and negative activations of
256 the cluster's centroid with a set of a priori defined functional 'communities' or networks
257 (Schaefer et al., 2018; Yeo et al., 2011). The results were visualized as spider plots for the
258 Schaefer atlases.

259 In further exploratory analyses, we describe the associations between brain state dy-
260 namics and other measures of cognitive ability such as memory and language.

Pilot data and analysis

262 Summary data from the first 1000 imaging data points of the HCHS have been published
263 with (Schlemm et al., 2022) and formed the basis for the hypotheses tested in this replication
264 study. Before preregistration, we had implemented our prespecified analysis pipeline described
265 above in R and Matlab, and applied it to this previous sample. Data, code and results

Timeline and access to data

269 At the time of planning of this study, all demographic, clinical and imaging data used in
270 this analysis had been collected by the HCHS and were held in the central trial database.
271 Quality checks for non-imaging variables had been performed centrally. WMH segmentation
272 based on structural MRI data of the first 10 000 participants of the HCHS had been performed
273 previously using the BIANCA/LOCATE approach (Rimmele et al., 2022). Functional MRI
274 data and clinical measures of executive dysfunction (TMT-B scores) had not previously
275 been analyzed by the pre-registering author (ES).

Deviations from preregistration

277 For deconfounding and aggregating BOLD data at brain parcellation level, the software
278 xcpEngine was used in version 1.2.3, not 1.2.1, to ensure that that the correct MNI ref-
279 erence template (MNI152NLin2009cAsym) is used for registration of brain atlases. This
280 decision was made before analysing the data.

Results

282 For this replication study, a total of 2648 datasets were available, of which 970 were al-
283 ready included in our previous analysis and thus discarded. In 13 of the resulting 1678
284 datasets, one or more MRI sequences were missing. Of the complete datasets (n=1665),
285 we excluded 5 participants due to intra-axial space-occupying lesions. An additional 9
286 ~~subjects~~ participants were excluded because of unsuccessful preprocessing, WMH seg-
287 mentation, or xcpEngine failure, resulting in 1651 datasets for analysis. A study-flowchart
288 is provided in Figure 2.

289 Baseline demographic and cognitive values, including the number of missing items,
290 are reported in Table 4.

291 WMH volumes (median 1.05 mL, IQR 0.47 mL to 2.37 mL), motion estimates, and frac-
292 tional occupancies of brain states 1 through 5 are reported in Table 5.

293 In an outcome-neutral quality check of the implementation of (i) the MRI processing
294 pipeline, (ii) brain state estimation, and (iii) co-activation pattern analysis, the mean differ-
295 ence in fractional occupancy between high- and low-occupancy states was consistently
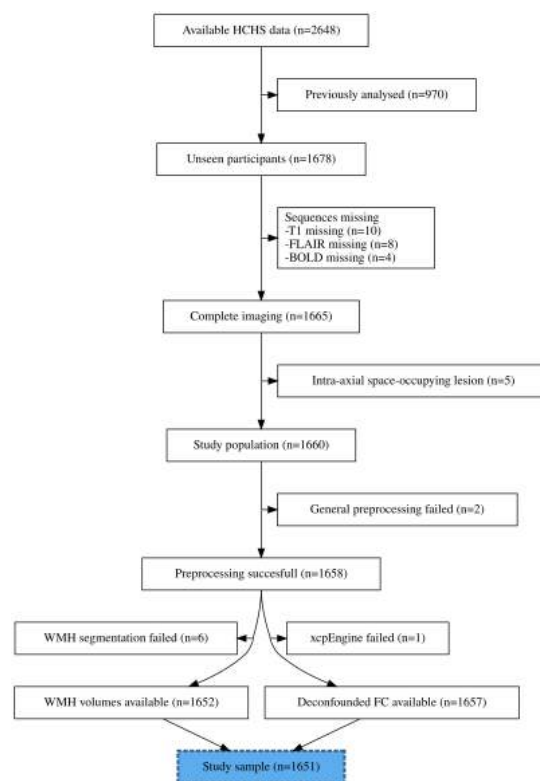
Figure 2 | **Study flowchart.** Composition of the study population after application of inclusion and exclusion criteria, and image processing.

296 maintained, with a point-estimate of the separation between two high-occupancy and

297 three low-occupancy states of 6.7% (95 % confidence interval, 6.2% to 7.1%) in the *36p*

298 paradigm. This indicates that the implementation of the pipeline was correct and that

299 the brain state estimation and co-activation pattern analysis worked as intended.

300 Pre-registered hypotheses

301 Association between WMH load and fractional occupancy

302 The results of the test of our primary preregistered hypothesis of an association be-

303 tween supratentorial WMH volume and the time spent in high-occupancy brain states

304 are shown in Figure 3 and Table 7.

305   Adjusted for age and sex, there was a 0.94-fold reduction in the odds of occupying a

306 high-occupancy brain state for every 5.1-fold increase in WMH load (P 5.01×10^{-8}).

307 Association between executive function and fractional occupancy in DMN-

308 related states

309 The results of the test of our secondary preregistered hypothesis of an association be-

310 tween time spent in high-occupancy brain states and executive function as measured by

311 the complete part B of the TMT are shown in Figure 4 and Table 9.

312   Adjusted for age, sex, WMH volume, and years of education, there was a 0.98-fold

313 reduction in the time to complete the TMT-B for every 5 % increase in the time spent in
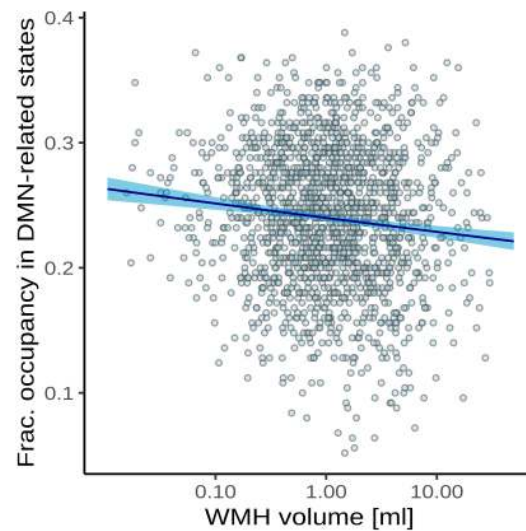
Figure 3 | Association between time spent in high-occupancy brain states and supratentorial WMH volume. Point estimates (black line) and 95%-confidence region (light blue ribbon) of the conditional mean fractional occupancy are obtained from unadjusted beta regression modelling. Each marker represents one of N=1642 independent participants with a non-zero total WMH volume.
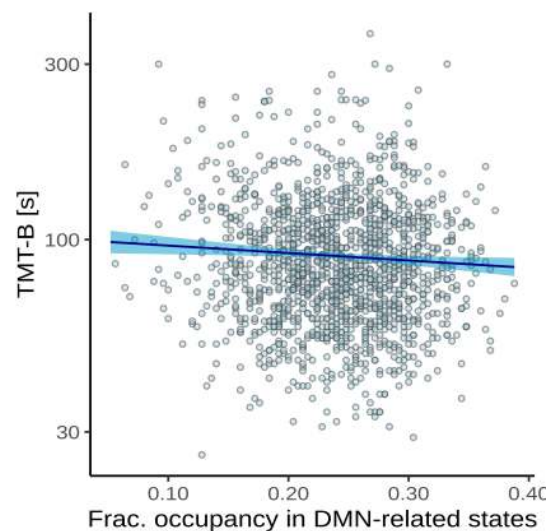
Figure 4 | Association between time spent in high-occupancy DMN-related brain states and TMT-B completion time. Point estimates (black line) and 95%-confidence region (light blue ribbon) of the conditional mean TMT-B completion time are obtained from unadjusted Gamma regression modelling. Each marker represent one of N=1482 independent participants with non-zero total WMH volume and available TMT-B data.

icant negative and no significant positive associations, irrespective of operationalization of cSVD (total vs. periventricular vs. deep WMH volume) (Figure 5B).

Additional analyses

Connectivity profiles of brain states – relation to default mode network

Based on the cosine similarity between positive and negative activations of cluster centroids and indicator vectors of pre-defined large scale brain networks, network activation profiles were computed for brain states estimated from Schaefer parcellations of varying spatial ~~resolution~~resolutions.

Figure 6 shows the corresponding spider plots, identifying states characterized by activation (DMN+) or suppression (DMN-) of the default mode network as states with the highest fractional occupancy.

Association with other cognitive domains

Associations between the time spent in high-occupancy DMN-related brain states and cognitive measures beyond TMT-B are shown in Figure 7.

Adjusted for age, sex, WMH load, and years of education, FO in DMN-related states appeared to be associated with better word recall (~~aOR~~ adjusted OR 1.19, nominal P 0.013), but not with global cognitive functioning (MMSE, ~~aOR~~ adjusted OR 1.09) or vocabulary (aOR 1.09), nor with verbal fluency (animal naming, adjusted $\exp(\beta)$ 1.04), or pure processing speed (TMT-A, adjusted $\exp(\beta)$ 0.97).

Summary and Discussion

In this pre-registered cross-sectional study we replicated the key findings of Schlemm et al., 2022 in an independent population-based sample of 1651 middle-aged to elderly participants of the Hamburg City Health Study.

First, we confirmed that the severity of cerebral small vessel disease is associated with the time spent in high-occupancy brain states, defined by functional MRI. More precisely, we showed that every 5.1-fold increase in the volume of supratentorial white matter hyperintensities of presumed vascular origin (WMH) was associated with a 0.95-fold reduction in the odds of occupying a brain state characterized by activation or suppression of the default-mode network, at any given time during the resting-state scan.

Second, we confirmed that the time spent in high-occupancy brain states at rest is associated with cognitive performance. More precisely, a 5%-reduction in the fractional
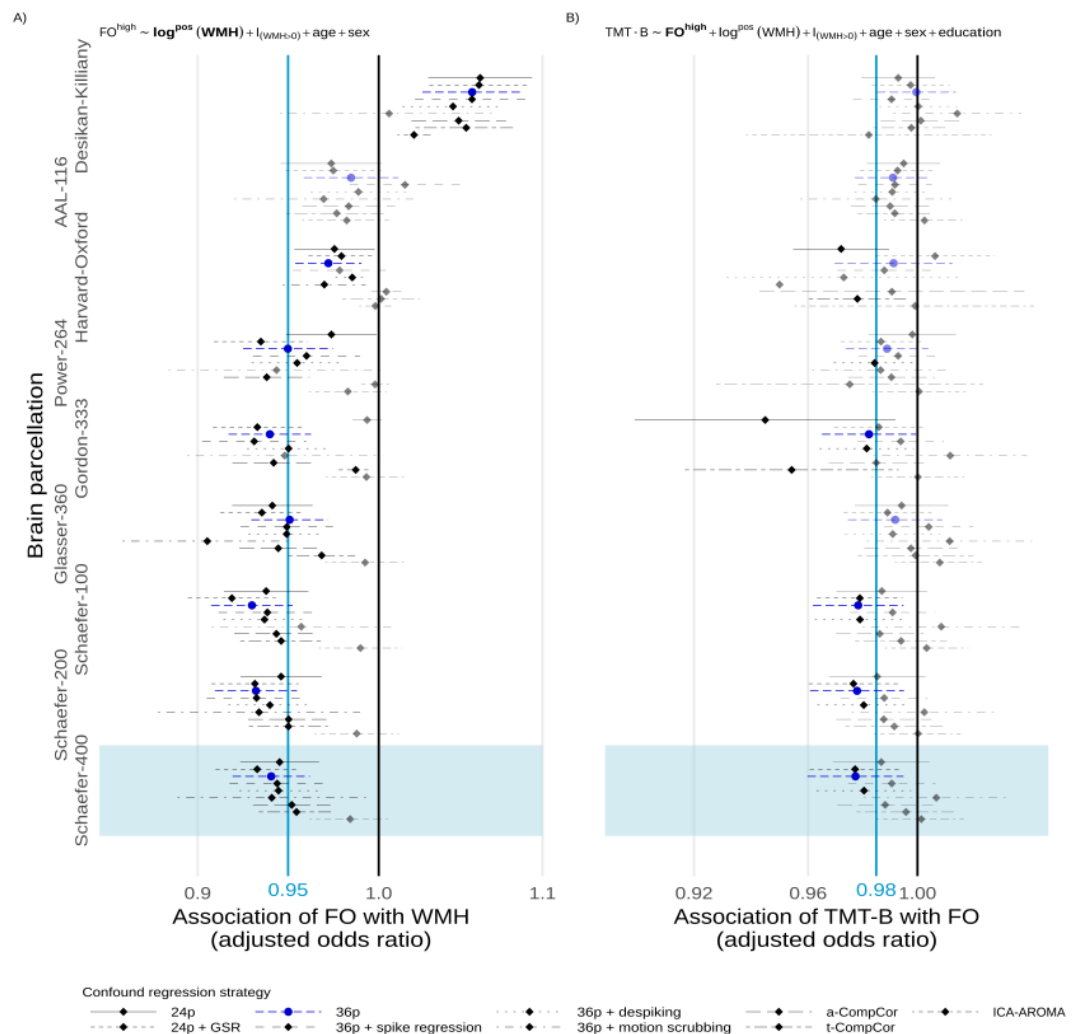
Figure 5 | Multiverse analysis. Adjusted effect size estimates of the associations between cSVD severity (WMH volume) and network dedifferentiation (less time spent in high-occupancy DMN-related brain states) [**A)**], and between network dedifferentiation and executive function (TMT-B completion time) [**B)**]. Effect sizes are given per 5.1-fold increase in WMH volume and a 5%-increase in fractional occupancy, respectively. Markers and line segments indicate point estimates and 95%-confidence intervals for adjusted odds ratios for different combinations of confound regression strategy and brain parcellation. The primary analytical choices are indicated by dark blue circles (36p) and light blue shading (Schaefer-400). Model equations for beta and gamma regressions, respectively, are given at the top. Vertical lines indicate no effect (black) and the effect size observed in the discovery cohort (Schlemm et al., 2022) (light blue), respectively, for reference. Effect sizes not reaching nominal statistical significance ($\alpha = 0.05$) are shown desaturated. Corresponding data based on periventricular and deep WMH volumes are presented in the Supplementary Appendix.
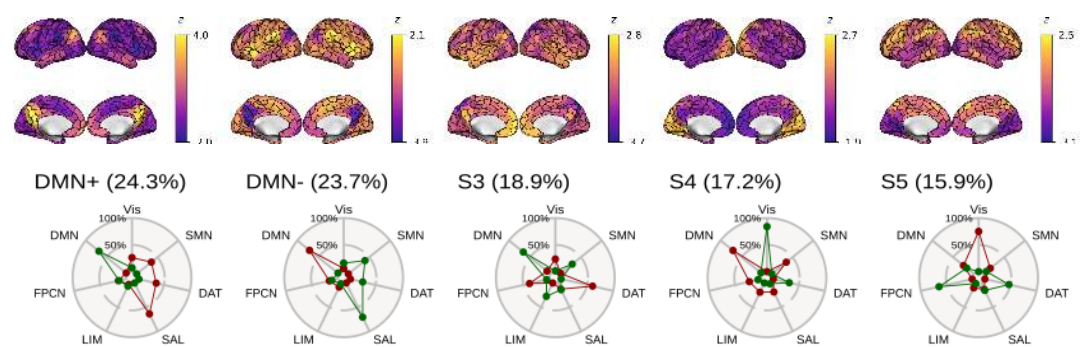
Figure 6 | **Connectivity profiles of brain states.** [**Top**] Centroids of each identified brain state visualized in brain space. Note the individual color scales. [**Bottom**] Cosine similarity between centroids of brain states and signed indicator vectors corresponding to activation (green) and suppression (red) of each of seven predefined large-scale functional brain networks (Yeo et al., 2011).

States are ordered by mean fractional occupancy across N=1651 independent participants, indicated by parenthetical percentages. Two high-occupancy states are characterized by activation or suppression of the DMN, the remaining three low-occupancy states (S3–5) were not used in the present study. Note that mean FO values are similar, but not identical, to median FO values reported in Table 5.

358 occupancy of DMN-related brain states was associated with a 1.02-fold increase in the

359 time to complete part B of the trail making test (TMT).

360 In a pre-planned multiverse analysis, ~~these findings~~ findings relating to our primary

361 and, to a lesser extent, secondary hypotheses were robust with respect to variations in

362 brain parcellations and confound regression strategies. Inconsistent results were found

363 with the Desikan–Killiany parcellation, likely reflecting the notion that the spatial resolu-

364 tion and functional specificity of this coarse, structurally defined atlas are inadequate for

365 analyzing functionally defined brain states. Across brain parcellations, effect sizes were

366 smaller with the ICA-AROMA confound regression strategy and failed to reach nominal

367 statistical significance. This might be due to a relatively large residual motion compo-

368 nent in measures of dynamical functional Connectivity after de-noising with ICA-AROMA,

369 as described previously (Lydon-Staley et al., 2019).

370 We also confirmed across several brain parcellation resolutions that high-occupancy

371 states at rest are characterized by either activation or suppression of the default mode

372 network, reflecting its role as the predominant task-negative brain network.

373 In unplanned, exploratory analyses, we described the association between brain state

374 dynamics and cognitive measures other than executive function and processing speed

375 and reported a strong, preliminary association between time spent in high-occupancy

376 states and delayed word recall.
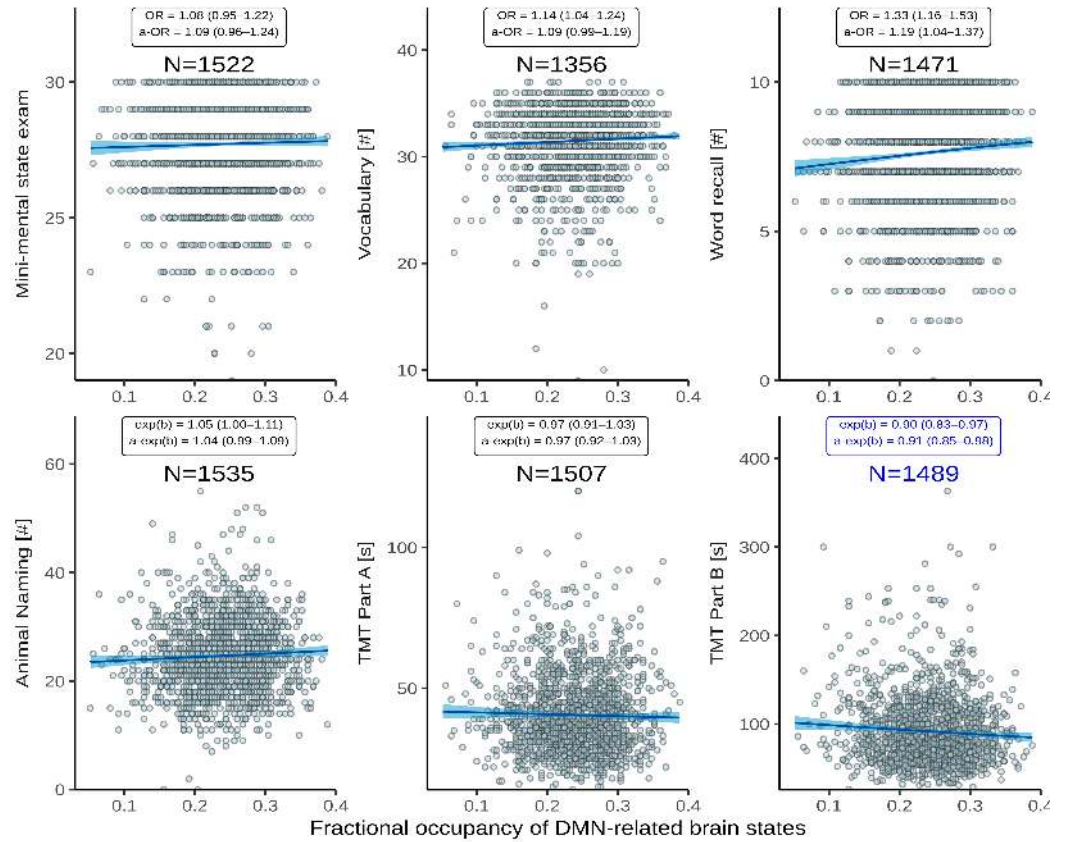
Figure 7 | **Association between time spent in high-occupancy DMN-related brain states and cognitive measures.** Point estimates (black line) and 95%-confidence region (light blue ribbon) of the conditional mean cognitive measures are obtained from unadjusted binomial (top row: Mini-Mental State Examination, Vocabulary, Word List Recall, logit link) and Gamma regression (bottom row: Animal Naming, Trail Making Test [TMT] A/B: log link) modelling. Each marker represents one of N independent participants, as indicated. Insets report effect sizes and P-values both with (adjusted [a-]) and without adjustment for the nuisance variables age, sex, WMH volume (coded as in Figure 5), and years of education. Effect sizes were quantified as odds ratios (ORs) (top) or response scale multipliers [exp(b)] (bottom), and correspond to a 20%-increase in fractional occupancy. Note the different reference change in FO compared to Table 9 chosen to adequately represent some of the smaller effect sizes. The bottom right panel highlighted in dark blue reproduces Figure 4.

We further explored, ~~but did not report in detail~~and report in the Supplementary appendix, the effect of motion; ~~all reported associations~~ results relating to our primary and, to a lesser extent, secondary, hypotheses were robust to additional, unplanned adjustments for DVARS, RMSD~~or~~, and mean framewise displacement.

The presented results provide robust evidence for a behaviorally relevant association between cerebral small vessel disease and functional brain network dedifferentiation.

Further research is required to replicate our findings in different populations, such as those affected more severely by cSVD or cognitive impairment, or being studied using different imaging protocols, to determine the generalizability of our findings with respect to varying operationalizations of the notions of cSVD, brain state, and cognition, and to understand the mechanisms underlying the reported associations.

Timeline and access to data

~~At the time of planning of this study, all demographic, clinical and imaging data used in this analysis had been collected by the HCHS and were held in the central trial database. Quality checks for non-imaging variables had been performed centrally. WMH segmentation based on structural MRI data of the first 10 000 participants of the HCHS had been performed previously using the BIANCA/LOCATE approach . Functional MRI data and clinical measures of executive dysfunction (TMT-B scores) had not previously been analyzed by the pre-registering author (ES).~~

Acknowledgment

This preprint was created using the LaPreprint template (https://github.com/roaldarbol/lapreprint) by Mikkel Roald-Arbøl ⓘ.

Disclosure

The authors of this article declare that they have no financial conflict of interest with the content of this article.

References

Arbuthnott, Katherine and Janis Frank (2000). "Trail making test, part B as a measure of executive control: validation using a set-switching paradigm". In: *Journal of clinical and experimental neuropsychology* 22.4, pp. 518–528.

406 Behzadi, Yashar et al. (2007). "A component based noise correction method (CompCor)
407   for BOLD and perfusion based fMRI". In: *Neuroimage* 37.1, pp. 90–101.

408 Bos, Daniel et al. (2018). "Cerebral small vessel disease and the risk of dementia: A sys-
409   tematic review and meta-analysis of population-based evidence". en. In: *Alzheimers.*
410   *Dement.* 14.11, pp. 1482–1492.

411 Cannistraro, Rocco J et al. (2019). "CNS small vessel disease: A clinical review". en. In: *Neu-*
412   *rology* 92.24, pp. 1146–1156.

413 Ciric, Rastko, Adon FG Rosen, et al. (2018). "Mitigating head motion artifact in functional
414   connectivity MRI". In: *Nature protocols* 13.12, pp. 2801–2826.

415 Ciric, Rastko, Daniel H Wolf, et al. (2017). "Benchmarking of participant-level confound
416   regression strategies for the control of motion artifact in studies of functional con-
417   nectivity". en. In: *Neuroimage* 154, pp. 174–187.

418 Cornblath, Eli J et al. (2020). "Temporal sequences of brain activity at rest are constrained
419   by white matter structure and modulated by cognitive demands". en. In: *Commun Biol*
420   3.1, p. 261.

421 Cox, Robert W (1996). "AFNI: software for analysis and visualization of functional mag-
422   netic resonance neuroimages". In: *Computers and Biomedical research* 29.3, pp. 162–
423   173.

424 Das, Alvin S et al. (2019). "Asymptomatic Cerebral Small Vessel Disease: Insights from
425   Population-Based Studies". en. In: *J. Stroke Cerebrovasc. Dis.* 21.2, pp. 121–138.

426 Desikan, Rahul S et al. (2006). "An automated labeling system for subdividing the human
427   cerebral cortex on MRI scans into gyral based regions of interest". In: *Neuroimage* 31.3,
428   pp. 968–980.

429 Dey, Ayan K et al. (2016). "Pathoconnectomics of cognitive impairment in small vessel
430   disease: A systematic review". en. In: *Alzheimers. Dement.* 12.7, pp. 831–845.

431 Esteban, Oscar et al. (2019). "fMRIPrep: a robust preprocessing pipeline for functional
432   MRI". en. In: *Nat. Methods* 16.1, pp. 111–116.

433 Frey, Benedikt M et al. (2021). "White matter integrity and structural brain network topol-
434   ogy in cerebral small vessel disease: The Hamburg city health study". en. In: *Hum. Brain*
435   *Mapp.* 42.5, pp. 1406–1415.

436 Friston, Karl J et al. (1996). "Movement-related effects in fMRI time-series". In: *Magnetic*
437   *resonance in medicine* 35.3, pp. 346–355.

Gesierich, Benno et al. (2020). "Alterations and test-retest reliability of functional connectivity network measures in cerebral small vessel disease". en. In: *Hum. Brain Mapp.* 41.10, pp. 2629–2641.

Glasser, Matthew F et al. (2016). "A multi-modal parcellation of human cerebral cortex". en. In: *Nature* 536.7615, pp. 171–178.

Gordon, Evan M et al. (2016). "Generation and Evaluation of a Cortical Area Parcellation from Resting-State Correlations". en. In: *Cereb. Cortex* 26.1, pp. 288–303.

Griffanti, Ludovica, Mark Jenkinson, et al. (2018). "Classification and characterization of periventricular and deep white matter hyperintensities on MRI: A study in older adults". en. In: *Neuroimage* 170, pp. 174–181.

Griffanti, Ludovica, Giovanna Zamboni, et al. (2016). "BIANCA (Brain Intensity AbNormality Classification Algorithm): A new tool for automated segmentation of white matter hyperintensities". en. In: *Neuroimage* 141, pp. 191–205.

Jagodzinski, Annika et al. (2020). "Rationale and Design of the Hamburg City Health Study". en. In: *Eur. J. Epidemiol.* 35.2, pp. 169–181.

Laumann, Timothy O, Evan M Gordon, et al. (2015). "Functional system and areal organization of a highly sampled individual human brain". In: *Neuron* 87.3, pp. 657–670.

Laumann, Timothy O and Abraham Z Snyder (2021). "Brain activity is not only for thinking". In: *Current Opinion in Behavioral Sciences* 40, pp. 130–136.

Laumann, Timothy O, Abraham Z Snyder, et al. (2017). "On the stability of BOLD fMRI correlations". In: *Cerebral cortex* 27.10, pp. 4719–4732.

Lawrence, Andrew J, Ai Wern Chung, et al. (2014). "Structural network efficiency is associated with cognitive impairment in small-vessel disease". en. In: *Neurology* 83.4, pp. 304–311.

Lawrence, Andrew J, Daniel J Tozer, et al. (2018). "A comparison of functional and tractography based networks in cerebral small vessel disease". en. In: *Neuroimage Clin* 18, pp. 425–432.

Lawrence, Andrew J, Eva A Zeestraten, et al. (2018). "Longitudinal decline in structural networks predicts dementia in cerebral small vessel disease". en. In: *Neurology* 90.21, e1898–e1910.

Lydon-Staley, David M et al. (2019). "Evaluation of confound regression strategies for the mitigation of micromovement artifact in studies of dynamic resting-state func-

tional connectivity and multilayer network modularity". In: *Network Neuroscience* 3.2, pp. 427–454.

Macey, Paul M et al. (2004). "A method for removal of global effects from fMRI time series". In: *Neuroimage* 22.1, pp. 360–366.

Makris, Nikos et al. (2006). "Decreased volume of left and total anterior insular lobule in schizophrenia". In: *Schizophrenia research* 83.2-3, pp. 155–171.

Muschelli, John et al. (2014). "Reduction of motion-related artifacts in resting state fMRI using aCompCor". In: *Neuroimage* 96, pp. 22–35.

Petersen, Marvin et al. (2020). "Network Localisation of White Matter Damage in Cerebral Small Vessel Disease". en. In: *Sci. Rep.* 10.1, p. 9210.

Power, Jonathan D, Alexander L Cohen, et al. (2011). "Functional network organization of the human brain". en. In: *Neuron* 72.4, pp. 665–678.

Power, Jonathan D, Anish Mitra, et al. (2014). "Methods to detect, characterize, and remove motion artifact in resting state fMRI". In: *Neuroimage* 84, pp. 320–341.

Prins, Niels D et al. (2005). "Cerebral small-vessel disease and decline in information processing speed, executive function and memory". en. In: *Brain* 128.Pt 9, pp. 2034–2041.

Pruim, Raimon HR et al. (2015). "ICA-AROMA: A robust ICA-based strategy for removing motion artifacts from fMRI data". In: *Neuroimage* 112, pp. 267–277.

Reijmer, Yael D et al. (2016). "Small vessel disease and cognitive impairment: The relevance of central network connections". en. In: *Hum. Brain Mapp.* 37.7, pp. 2446–2454.

Rimmele, David Leander et al. (2022). "Association of Carotid Plaque and Flow Velocity With White Matter Integrity in a Middle-aged to Elderly Population". en. In: *Neurology*.

Satterthwaite, Theodore D et al. (2013). "An improved framework for confound regression and filtering for control of motion artifact in the preprocessing of resting-state functional connectivity data". In: *Neuroimage* 64, pp. 240–256.

Schaefer, Alexander et al. (2018). "Local-Global Parcellation of the Human Cerebral Cortex from Intrinsic Functional Connectivity MRI". en. In: *Cereb. Cortex* 28.9, pp. 3095–3114.

Schlemm, Eckhard et al. (2022). "Equalization of Brain State Occupancy Accompanies Cognitive Impairment in Cerebral Small Vessel Disease". en. In: *Biol. Psychiatry* 92.7, pp. 592–602.

Schulz, Maximilian et al. (2021). "Functional connectivity changes in cerebral small vessel disease - a systematic review of the resting-state MRI literature". en. In: *BMC Med.* 19.1, p. 103.

Shen, Jun et al. (2020). "Network Efficiency Mediates the Relationship Between Vascular Burden and Cognitive Impairment: A Diffusion Tensor Imaging Study in UK Biobank". en. In: *Stroke* 51.6, pp. 1682–1689.

Steegen, Sara et al. (2016). "Increasing Transparency Through a Multiverse Analysis". en. In: *Perspect. Psychol. Sci.* 11.5, pp. 702–712.

Sundaresan, Vaanathi et al. (2019). "Automated lesion segmentation with BIANCA: Impact of population-level features, classification algorithm and locally adaptive thresholding". en. In: *Neuroimage* 202, p. 116056.

Tombaugh, Tom N (2004). "Trail Making Test A and B: normative data stratified by age and education". en. In: *Arch. Clin. Neuropsychol.* 19.2, pp. 203–214.

Tuladhar, Anil M, Ewoud van Dijk, et al. (2016). "Structural network connectivity and cognition in cerebral small vessel disease". en. In: *Hum. Brain Mapp.* 37.1, pp. 300–310.

Tuladhar, Anil M, Jonathan Tay, et al. (2020). "Structural network changes in cerebral small vessel disease". en. In: *J. Neurol. Neurosurg. Psychiatry* 91.2, pp. 196–203.

Tzourio-Mazoyer, Nathalie et al. (2002). "Automated anatomical labeling of activations in SPM using a macroscopic anatomical parcellation of the MNI MRI single-subject brain". In: *Neuroimage* 15.1, pp. 273–289.

Vidaurre, Diego et al. (2018). "Discovering dynamic brain networks from big data in rest and task". en. In: *Neuroimage* 180.Pt B, pp. 646–656.

Wardlaw, Joanna M, Colin Smith, and Martin Dichgans (2013). "Mechanisms of sporadic cerebral small vessel disease: insights from neuroimaging". en. In: *Lancet Neurol.* 12.5, pp. 483–497.

Wardlaw, Joanna M, Eric E Smith, et al. (2013). "Neuroimaging standards for research into small vessel disease and its contribution to ageing and neurodegeneration". en. In: *Lancet Neurol.* 12.8, pp. 822–838.

Wardlaw, Joanna M, Maria C Valdés Hernández, and Susana Muñoz-Maniega (2015). "What are white matter hyperintensities made of? Relevance to vascular cognitive impairment". en. In: *J. Am. Heart Assoc.* 4.6, p. 001140.

Xu, Yuanhang et al. (2021). "Altered Dynamic Functional Connectivity in Subcortical Ischemic Vascular Disease With Cognitive Impairment". en. In: *Front. Aging Neurosci.* 13, p. 758137.

Yeo, B T Thomas et al. (2011). "The organization of the human cerebral cortex estimated by intrinsic functional connectivity". en. In: *J. Neurophysiol.* 106.3, pp. 1125–1165.

536 Yin, Wenwen et al. (2022). "The Clustering Analysis of Time Properties in Patients With
537 Cerebral Small Vessel Disease: A Dynamic Connectivity Study". en. In: *Front. Neurol.*
538 13, p. 913241.

Question	Hypothesis	Sampling plan	Analysis plan	Rationale for deciding the sensitivity of the test	Interpretation given different outcomes	Theory that could be shown wrong by the outcome
Is severity of cerebral small disease, quantified by the volume of supratentorial white matter hyperintensities of presumed vascular origin (WMH), associated with time spent in high-occupancy brain states, defined by resting-state functional MRI?	**(Primary)** Higher WMH volume is associated with lower average occupancy of the two highest-occupancy brain states.	Available ~~subjects~~ participants with clinical and imaging data from the the HCHS (Jagodzinski et al., 2020)	Standardized preprocessing of structural and functional MRI data • automatic quantification of WMH • co-activation pattern analysis • multivariable generalised regression analyses	Tradition	$P < 0.05$ –> rejection of the null hypothesis of no association between cSVD and fractional occupancy; $P > 0.05$ –> insufficient evidence to reject the null hypothesis	Functional brain dynamics are not related to subcortical ischemic vascular disease.
Is time spent in high-occupancy brain states associated with cognitive impairment, measured as the time to complete part B of the trail making test (TMT)?	**(Secondary)** Lower average occupancy of the two highest-occupancy brain states is associated with longer TMT-B time.	as above	as above	as above	$P < 0.05$ –> rejection of the null hypothesis of no association between fractional occupancy and cognitive impairment; $P > 0.05$ –> insufficient evidence to reject the null hypothesis	Cognitive function is not related to MRI-derived functional brain dynamics.

Table 1 | Study Design Template. Overview of the Scientific Questions addressed in the present study (first column), the two main hypotheses being investigated (second column), and details of the underlying study.

Name of the atlas	#parcels	Reference
Desikan–Killiany	86	Desikan et al., 2006
AAL	116	Tzourio-Mazoyer et al., 2002
Harvard–Oxford	112	Makris et al., 2006
glasser360	360	Glasser et al., 2016
gordon333	333	Gordon et al., 2016
power264	264	Power, Cohen, et al., 2011
schaefer{N}	100	Schaefer et al., 2018
	200	
	400	

AAL: Automatic Anatomical Labelling

(a) Parcellations

Design	Reference
24p	Friston et al., 1996
24p + GSR	Macey et al., 2004
36p	Satterthwaite et al., 2013
36p + spike regression	Cox, 1996
36p + despiking	Satterthwaite et al., 2013
36p + scrubbing	Power, Mitra, et al., 2014
aCompCor	Muschelli et al., 2014
tCompCor	Behzadi et al., 2007
AROMA	Pruim et al., 2015

GSR: Global signal regression, AROMA: Automatic Removal of Motion Artifacts

(b) Confound regression strategies, adapted from (Ciric, Wolf, et al., 2017)

Table 2 | Multiverse analysis. Overview over different brain parcellations and confound regression strategies implemented using xcpEngine (Ciric, Rosen, et al., 2018). A total of $9 \times 9 = 81$ analytical combinations were explored to assess the robustness of our results with respect to these processing choices.

	N = 1,651
Demographics (no Missing n (%))	
Age, yr	
Median (IQR)	66 (59 – 72)
Sex	
Male	940/1651 (57%)
Female	711/1651 (43%)
Cardiovascular risk factors	
Hypertension	
Present	1177/1611 (73.1%)
Missing n (%)	85 (5.1%)
Diabetes	
Present	157/1566 (10%)
Missing n (%)	40 (2.4%)
Smoking	
Present	200/1360 (14.7%)
Missing n (%)	201 (12.9%%)
Hyperlipidaemia	
Present	426/1578 (27%)
Missing n (%)	73 (4.4%)
Cognitive test results	
MMSE, # (max. 30)	
Median (IQR)	28 (27 – 29)
Missing n (%)	129 (7.8%)
Vocabulary (MWT-B), # (max. 37)	
Median (IQR)	32 (30 – 34)
Missing n (%)	295 (18%)
Word recall, # (max. 10)	
Median (IQR)	8 (6 – 9)
Missing n (%)	180 (11%)
Animal Naming	
Median (IQR)	24 (20 – 29)
Missing n (%)	116 (7.0%)
TMT-A, seconds	
Median (IQR)	38 (31 – 48)
Missing n (%)	144 (8.7%)
TMT-B, seconds	
Median (IQR)	83 (65 – 110)
Missing n (%)	162 (9.8%)
History	
Diagnosed dementia	
Present	6/1645 (0.4%)
Missing n (%)	6 (0.4%)
Years of education	
Median (IQR)	13 (12 – 16)
Missing n (%)	34 (2%)

Table 4 | **Descriptive statistics of the study population.** Data are presented as median (interquartile range) or count (percentage) of non-missing items, as appropriate. Number of percentage of missing items are reported separately.

	N = 1,651
WMH volume[1], mL	
Total	1.05 (0.47 – 2.37), 9 Z
Periventricular	0.94 (0.43 – 2.04), 9 Z
Deep	0.10 (0.03 – 0.37), 344 Z
Motion during rs-fMRI	
Framewise displacement, mm	0.21 (0.15 – 0.63)
RMSD, mm	0.086 (0.058 – 0.12)
DVARS	27.8 (24.3 – 31.8)
Fractional occupancy, %	
DMN+	24.8 (20.8 – 28.0)
DMN-	24.0 (20.0 – 28.0)
S3	18.4 (15.2 – 22.4)
S4	16.8 (12.8 – 20.8)
S5	15.2 (12.0 – 19.2)

[1]Number of zero values indicated by Z

Table 5 | Structural and functional imaging characteristics. Data are presented as median (interquartile range). Supratentorial WMH volumes were obtained by semiautomatic segmentation of FLAIR images using a BINACA/LOCATE-based k-nearest neighbours algorithm and stratified by their distance to the lateral ventricles (<10 mm, periventricular; >10 mm, deep). Motion parameters were estimated during fMRIprep processing of BOLD scans. Fractional occupancies were calculated by assigning individual BOLD volumes to one of five discrete brain states defined by k-means clustering-based co-activation pattern analysis.Two high-occupancy states are labelled DMN+ and DMN- in view of their network connectivity profiles as shown in Figure 6.

	Estimate	P	95%-CI
Intercept	0.24	<0.0001	0.21 – 0.27
WMH, per 5.1-fold increase[1]	0.94	<0.0001	0.92 – 0.96
Age, per 10 years	1.04	0.001	1.01 – 1.06
Female sex	1.12	<0.0001	1.09 – 1.16
$\mathbf{1}_{\{WMH=0\}}$	0.93	0.477	0.75 – 1.14

[1] Interquartile ratio $2.37/0.468 = 5.06$

Table 7 | Association between time-spent in high-occupancy DMN-related brain states and WMH volume adjusted for age and sex. Beta regression table estimated from $n = 1651$ independent participants using the model equation $FO^{high} \sim \log WMH^+ + \mathbf{1}_{\{WMH=0\}} + age + sex$.

	Estimate	P	95%-CI
Intercept	53.41	< 0.0001	42.7 – 66.8
FO^{high}, per 5%	0.98	0.0116	0.96 – 0.99
WMH, per 5.1-fold increase[1]	1.01	0.367	0.98 – 1.05
Age, per 10 years	1.18	<0.0001	1.15 – 1.21
Female sex	0.99	0.666	0.95 – 1.03
Education, per year	0.97	<0.0001	0.97 – 0.98
$\mathbf{1}_{\{WMH=0\}}$	0.97	0.398	0.92 – 1.03

[1] Interquartile ratio $2.37/0.468 = 5.06$

Table 9 | Association between TMT-B and time spent in high-occupancy DMN-related brain states adjusted for age, sex, WMH volume and years of education. Gamma regression table estimated from $n = 1483$ independent participants using the model equation
$TMT{-}B \sim FO^{high} + \log WMH^{+} + \mathbf{1}_{\{WMH=0\}} + age + sex + education years.$

Supplementary results

Deep and periventricular WMH

Here we present, in analogy to Figure 5, the results of the multiverse analyses of the association between cSVD burden, FO of DMN-related states, and executive function, when cSVD is operationalized as the volume of deep or periventricular white matter hyperintensities, respectively.
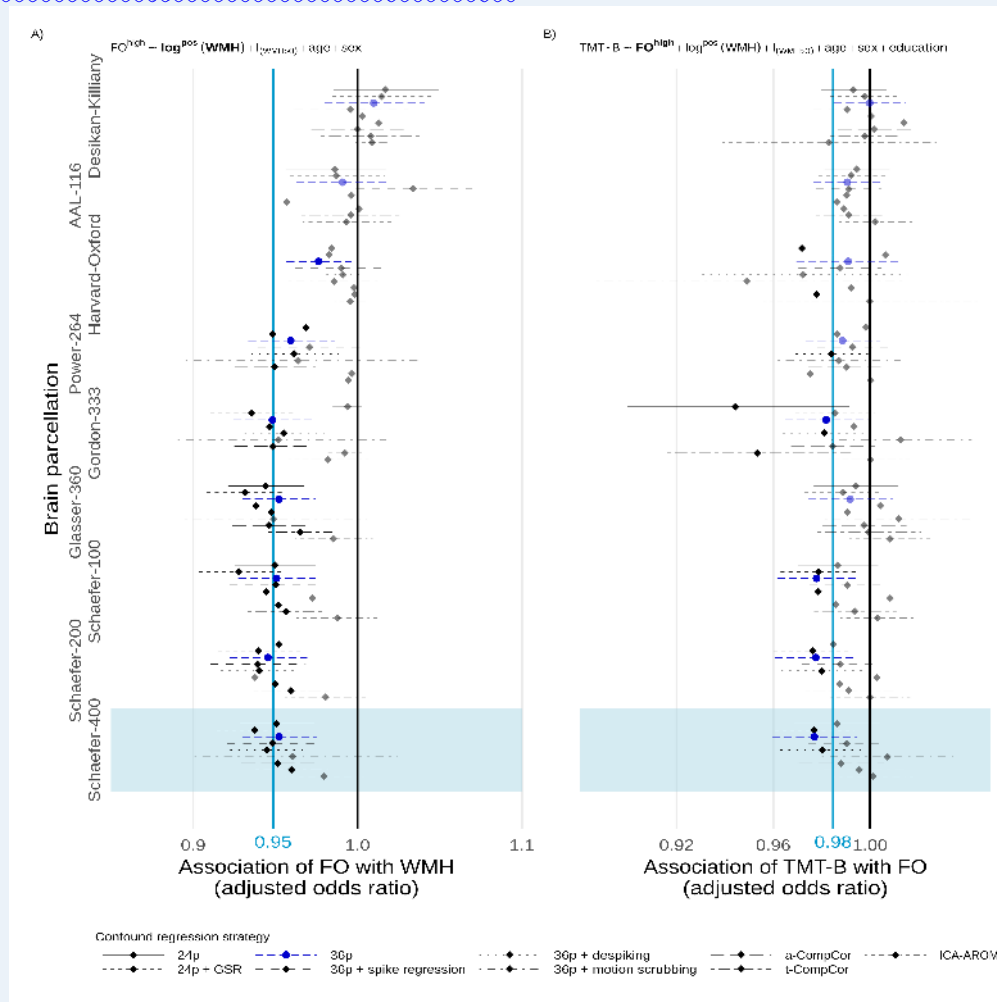
Appendix 1—figure 1 Multiverse analysis, deep WMH
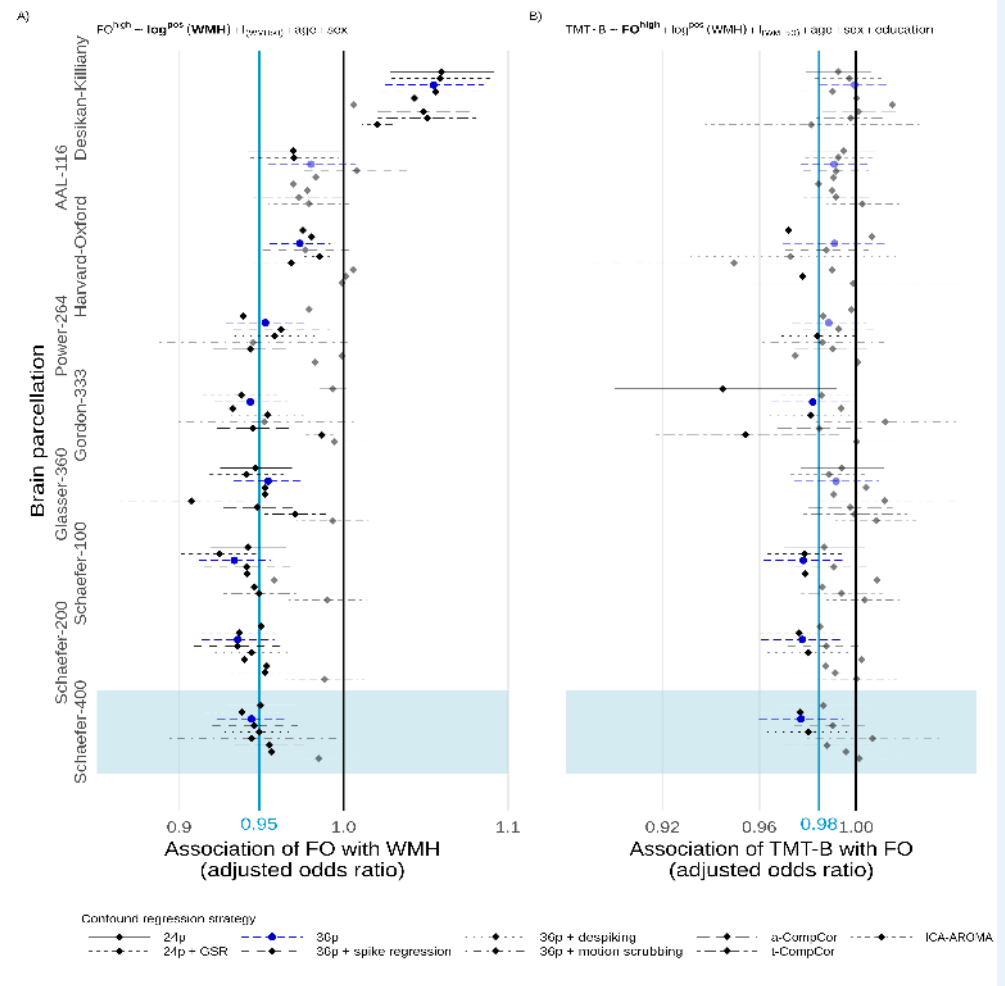
Appendix 1—figure 2 Multiverse analysis, periventricular WMH

Motion parameters

We also present, in analogy to Tables 7 and 9, regression tables for the association between time spent in DMN-related brain states (FO) and WMH volume, and between TMT-B and FO, adjusted for DVARS, RSMD and framewise displacement, in addition to age, sex and, in the latter case, years of education.

	Estimate	P	95%-CI
Intercept	0.32	<0.0001	0.28 – 0.36
WMH, per 5.1-fold increase[1]	0.96	0.0004	0.94 – 0.98
Age, per 10 years	1.01	<0.0001	1.00 – 1.01
Female sex	1.11	<0.0001	1.08 – 1.15
1{WMH=0}	0.91	0.3552	0.74 – 1.11

	0.98	<0.0001	0.98 – 0.99
DVARS	0.98	<0.0001	0.98 – 0.99
RMSD	28.29	0.0055	2.67 – 299.84
Framewise displacement	0.16	0.0112	0.04 – 0.66

[1] Interquartile ratio 2.37/0.468 = 5.06

Appendix 1—table 2 Association between time-spent in high-occupancy DMN-related brain states and WMH volume adjusted for age, sex, and **motion parameters**

	Estimate	P	95%-CI
Intercept	46.83	<0.0001	36.74 – 59.72
FO^{high}, per 5%	0.71	0.0718	0.49 – 1.03
WMH, per 5.1-fold increase[1]	1.01	0.3414	0.98 – 1.04
Age, per 10 years	1.02	<0.0001	1.01 – 1.02
Female sex	1.00	0.8171	0.96 – 1.04
Education, per year	0.97	<0.0001	0.97 – 0.98
$1_{\{WMH=0\}}$	0.96	0.7581	0.73 – 1.29
DVARS	1.01	0.0001	1.00 – 1.01
RMSD	0.31	0.4695	0.01 – 7.45
Framewise displacement	1.08	0.9322	0.16 – 7.13

[1] Interquartile ratio 2.37/0.468 = 5.06

Appendix 1—table 4 Association between TMT-B and time spent in high-occupancy DMN-related brain states adjusted for age, sex, WMH volume and years of education, and **motion parameters**